



Assessing the hydrogeological resilience of a groundwater-dependent Mediterranean peatland: Impact of global change and role of water management strategies

S. Santoni, E. Garel, M. Gillon, V. Marc, J. Miller, M. Babic, R. Simler, Y. Travi, M. Leblanc, F. Huneau

► To cite this version:

S. Santoni, E. Garel, M. Gillon, V. Marc, J. Miller, et al.. Assessing the hydrogeological resilience of a groundwater-dependent Mediterranean peatland: Impact of global change and role of water management strategies. Science of the Total Environment, 2021, 768, pp.144721. 10.1016/j.scitotenv.2020.144721 . hal-03549220

HAL Id: hal-03549220

<https://hal.science/hal-03549220v1>

Submitted on 3 Feb 2023

HAL is a multi-disciplinary open access archive for the deposit and dissemination of scientific research documents, whether they are published or not. The documents may come from teaching and research institutions in France or abroad, or from public or private research centers.

L'archive ouverte pluridisciplinaire **HAL**, est destinée au dépôt et à la diffusion de documents scientifiques de niveau recherche, publiés ou non, émanant des établissements d'enseignement et de recherche français ou étrangers, des laboratoires publics ou privés.



Distributed under a Creative Commons Attribution - NonCommercial 4.0 International License

Assessing the hydrogeological resilience of a groundwater-dependent Mediterranean peatland: impact of global change and role of water management strategies

S. SANTONI^{1,2,3,*}, E. GAREL^{1,2}, M. GILLON³, V. MARC³, J. MILLER⁴, M. BABIC³, R.
SIMLER³, Y. TRAVI³, M. LEBLANC³, F. HUNEAU^{1,2}.

¹Université de Corse Pascal Paoli, Faculté des Sciences et Techniques, Département
d'Hydrogéologie, Campus Grimaldi, BP 52, F-20250 Corte, France.

²CNRS, UMR 6134 SPE, F-20250 Corte, France.

³Avignon Université, UMR 1114 EMMAH, UAPV, 301 rue Baruch de Spinoza, BP 21239, F-84916
Avignon, France.

⁴Stellenbosch University, Department of Earth Sciences Private Bag XI, Matieland, 7602 South Africa.

(*) Corresponding author: Université de Corse Pascal Paoli, Faculté des Sciences et Techniques,
Département d'Hydrogéologie, CNRS, UMR 6134 SPE, Campus Grimaldi, BP 52, F-20250 Corte,
France. santoni_s@univ-corse.fr ; santonisebastien17@gmail.com ; Tel. +33635175342 ; Fax.
+33420202363

Acknowledgments

The postdoctoral grant of Sébastien Santoni and accompanying research action are financially supported by the “Culletività di Corsica” through the GERHYCO interdisciplinary project dedicated to water management, ecology, and hydro-ecosystem services in insular context. The authors would like to thank the Municipality of Moltifau and the forest managers from the ONF (Office National des Forêts) for their support and contribution to the implementation of the project. The authors acknowledge Guillaume Chevalier for the help provided during the field campaigns and André Renucci for the Moltifau rainwater monthly sampling.

Keywords

Watershed; Hydrogeology; Isotope Hydrology; Recharge; Integrated Water Resource Management; Corsica.

1. Introduction

Wetlands are essential for humankind as they provide food security and climate change mitigation through ecosystem services such as water regulation and biodiversity conservation. Peatlands, which make up an integral component of wetlands, are also known for significant carbon storage capacity through peat accumulation. During the period 1970-2013, the area of wetland worldwide decreased by 35%. This loss was more pronounced in the Mediterranean, with up to 48 % of wetland surface loss (Gardner et al., 2018) in spite of the fact that wetlands constitute biodiversity and endemism hotspots. The drastic wetland surface loss is mainly attributed to water withdrawal and agricultural land extension (Parish et al., 2008; Kløve et al., 2011; Malek et al., 2018). The aridity of the Mediterranean climate implies wetlands such as peatlands are expected to be threatened by ongoing and future climate change impacts. Extended drought periods may involve a decrease in the water table, enhancing mineralization of organic matter and turning these peatlands into a source of carbon and drylands (Urák et al., 2017; Huang et al., 2018).

The crucial need to preserve such peatlands is reflected by a large number of regional to supranational governmental and non-governmental initiatives promoting the need for sustainable development. These include the United Nations Convention to Combat Desertification (UNCCD, 1992), the Paris Climate Agreement (2015), the

United Nations Sustainable Development Goals (SDGs, 2015) and more specifically the Ramsar Convention (1971), the MedWet Mediterranean Wetlands Initiative (1991) and the Aichi biodiversity targets (2010). In concrete terms, these initiatives aim to identify and mitigate human pressures on the environment. All of them point out that it is critical to obtain detailed knowledge for each site, and specifically on geomorphological, geohydrological and hydroclimatic conditions that are by definition interconnected. It is therefore essential to develop strategies and methodologies able to identify the boundary conditions necessary to sufficiently understand peatlands functioning at the hydrosystem scale. This crucial step will guide sustainable development strategies and help to design integrated water resource management procedures to protect these wetlands and preserve their ecological value (Vlachopoulou et al., 2014; Hettiarachchi et al., 2015; Erostate et al., 2020).

Although peatlands are present in most of the countries bordering the Mediterranean Sea, they remain seriously under-investigated: not all are inventoried, their spatial extent and functioning are not properly reported and recharge mechanisms are largely unknown. What knowledge does exist, suggests Mediterranean peatlands are shaped by their local environment, making them small, scattered, and with most presumed to be groundwater-dependent (Finlayson et al., 2018). Nevertheless, peat and gley soils extend over approximately 64,000 km² over the Mediterranean, which means peatlands may cover up to 29 to 42 % of the total known wetland surface (Parish et al., 2008; Gardner et al., 2018). Thus additional information on the peatlands could help delineate their hydrological vulnerability and resilience capacity to climate change.

One of the most important knowledge gaps is in characterization and quantification of the water balance components necessary for biodiversity conservation and peat

accumulation. Peat accumulation occurs through the maintenance of water levels close to the surface irrespective of seasonal climate variation and over the long term, especially under the semi-arid conditions that characterise the Mediterranean area. Approaches combining complementary methods such as water level monitoring, hydrogeochemistry, and isotope hydrology tools have been widely employed to characterize the origin, periodicity, and recharge mechanisms of very large and well-developed wetlands mainly in cold humid climates (Howie and Van Meerveld, 2013; Isokangas et al., 2017). The same approach to investigation of more seasonal and inhomogeneous recharge mechanisms of Mediterranean peatlands is largely missing.

In this study, the Moltifau peatland on the island of Corsica (France) was investigated to characterize the seasonal recharge mechanisms of a low-altitude Mediterranean peatland exposed to extended low precipitation period during the summer. Water level monitoring was combined with major ion hydrochemistry as well as ^{18}O , ^2H , ^3H , and $^{87}\text{Sr}/^{86}\text{Sr}$ isotopes to identify and quantify complex water flows supplying a hydrosystem connected to a larger watershed. The results are used to evaluate the vulnerability and hydrogeological resilience of Mediterranean peatlands based on the origin and renewal dynamics of water bodies contributing to their recharge. Finally, the results are evaluated against existing water and aquatic environmental management policy frameworks. Effective policies are essential to protect the hydrogeological functioning of Mediterranean peatlands and in particular their potential vulnerability to future climate change.

2. Study site

76 The Moltifau peatland was selected for its strategic location in Corsica (France), a
77 mountainous island in the western Mediterranean basin. According to the Köppen
78 climate classification (Peel et al., 2007), Corsican coastal regions are characterized
79 by a Csa climate (hot-summer), mid-mountain regions by a Csb climate (warm-
80 summer), and small areas of highest altitude by a subarctic Dfc climate (snow with
81 dry and cool summer). Such a Mediterranean hydroclimatic context also implies
82 strong inter-seasonal and inter-annual heterogeneity of temperature and rainfall
83 conditions. Corsica is therefore an excellent observatory island giving access to all
84 continental hydrological processes on a small spatial scale.

85 The Moltifau peatland, which extends over 40,000m², lies on an alluvial plain
86 between 240 and 270 m a.s.l, within the Ascu River valley, an alpine watershed of
87 365 km² reaching a maximum elevation of 2706 m. a.s.l. Its inland location at low
88 altitude implies a Csb climate with severe summer drought conditions, the intensity,
89 and duration of which are continuously increasing due to climate change which in
90 turn increases the risk of the peatland drying out. The peatland is delimited by the
91 Ascu River at the north, and by the Punta di Ciufellu massif (820 m. a.s.l.) at the
92 south. The average annual temperature is 14.4°C (from +4°C in winter to +25 °C in
93 summer), and the average annual rainfall amount is 726 mm (from 13 mm in summer
94 to 99 mm in fall). The Ascu River has a torrential regime with a mean annual flow of
95 about 5.1 m³/s, from 0.8 m³/s in summer to 8.9 m³/s in fall. The Ascu regime is also
96 influenced by the high altitude Dfc climate involving spring snowpack melting
97 contribution to the flow. Private housing settlements, which are part of the alluvial
98 plain upstream, extend to the west of the peatland (Figure 1). Over the Moltifau area,
99 population and urbanism are growing strongly, by around +56% in 49 years and
100 +245% in 47 years, respectively. The drinking water supply mainly comes from the

101 Ascu River (upstream of the peatland) and numerous private boreholes pump the
102 alluvial groundwater for crop production.

103 The peatland shelters a high plant and animal biodiversity including species
104 protected at National, European, and International levels as well as several endemic
105 species justifying its internationally recognized ecological value (Reille, 1997;
106 Burguet-Moretti et al., 2011). It is referenced as the largest active raised bog on
107 Corsica, is mainly acidic (pH ~4-5), young (^{14}C dating ~ 515 +/- 45 years), and of little
108 thickness (1 to 2.5 m). Although there are some residues remaining from past landfill
109 activities around the alder forest (glass, rubble, and car bodies), the peatland area
110 itself can be considered as “pristine” (Poher, 2017). However, the peatland area is
111 not delimited by any barrier, signage, or other physical materialization and most of
112 the inhabitants of the town of Moltifau consider the peatland as an unhealthy place
113 and underestimate its ecological value.

114 The peatland is underlain by well-fractured, pink perthitic granites that are part of the
115 Punta di Ciufellu massif (Figure 1). Undifferentiated colluvium, resulting from the
116 erosion of the Ciufellu massif accumulates on its piedmont to a thickness of a few
117 meters and extends in the south of the peatland (Figure 1). The alluvial plain is made
118 of river alluvium organized in terraces of different ages deposited on the granitic
119 bedrock with a thickness of up to several tens of meters and permeability of about
120 6.4×10^{-4} m/s. Deposits consist mainly of more or less altered pebbles, nested in a
121 clayey orange paleosol close to the piedmont or a grey sandy matrix close to the
122 riverbed (Rossi et al., 1994).

123 Alder forest extending over 120,000 m² surrounds the peatland and hosts tiny
124 temporary streams supplied by runoff flows from the Ciufellu massif but also by
125 numerous cold-water springs on the ground. The cold-water springs origin is not

documented and probably related to the alluvial aquifer and colluvium discharge. The water level in the alluvial aquifer and the peatland displays little variation within the peatland irrespective of the season. The peatland is interpreted to be fed upstream by alluvial groundwater overflow due to a topographic threshold affecting alluvium terraces (Genevier et al., 2014).

3. Method

Five quarterly field surveys were conducted under contrasting hydrological conditions to represent a complete hydrological cycle from: May 2018 and June 2019 for spring, August 2018 for summer, December 2019 for fall, and February 2019 for winter. Data acquisition includes hourly monitoring of water level in the peatland (T4) and in the alluvial aquifer (F4) from June 2018 to June 2019. Secondly, it includes a monthly sampling for $\delta^{18}\text{O}$ and $\delta^2\text{H}$ of the river (R18) and Moltifau rainwater from May 2018 to June 2019 to constrain the local $\delta^{18}\text{O}$ variation. Thirdly, the data acquisition includes a quarterly survey for *in situ* measurements all over the study area of physico-chemical parameters (EC, HCO_3^-) and sampling for major ions (NO_3^- , Cl^- , SO_4^{2-} , Na^+ , Ca^{2+} , Mg^{2+} , K^+), stable isotopes of the water molecule ($\delta^{18}\text{O}$, $\delta^2\text{H}$), and tritium (^3H). A network of 25 points (Figure 1) was developed including the river (R18, R3, R7, R8), the alluvial aquifer (boreholes F1, F3, F4, F5, F7, F8; alder forest springs R10, R11, R12, R16, R19), the granitic massif (F6), the local rainwater (rain gauge near F6), the peatland water (piezometers T1, T2, T4, T5, T6) and its outlets (R1, R5, R6). Alluvial aquifer boreholes develop within the alluvium without reaching the granite bedrock, are not exploited and are used here as piezometers. Their depth increase with distance to the river: 5.7 m at F1, 3.0 m at F3, 6.7 m at F4, 8.2 at F5, 10 m at F8, 30 m at F7, and 103 m at F6. Peatland piezometers develop only within the peat, with a

depth of about 1.24 m at T1, 1.20 m at T2, 1.45 m at T4, 0.51 m at T5, and 1.27 m at T6. Water table elevation of the alluvial aquifer and the peatland is averaged between 247 and 253 m a.s.l during the studied period (Figure 1 and Figure 2). For the spring 2018 campaign, ^3H was not sampled. During the June-2019 campaign, a sample for dissolved inorganic radiocarbon ($^{14}\text{C}_{\text{DIC}}$) in F6 was collected, and strontium isotopes ($^{87}\text{Sr}/^{86}\text{Sr}$) were measured in 15 samples representative of all water bodies.

Water Electrical Conductivity (EC) and temperature were measured with a WTW Cond 3310 meter (WTW GmbH, Weilheim, Germany) in the field, and alkalinity was determined in the field using a HACH digital titrator (HACH Company, Loveland, USA). Water sampling was made after purging the piezometers (renewal of at least 3 times the volume of the water column) and stabilization of the physic-chemical parameters. Samples for major ions were filtered through 0.45 μm nitrocellulose membranes before collection in two 50 mL polyethylene bottles, with one of them acidified for cation analysis using ultrapure HNO_3 . A Dionex ICS 1100 chromatography (Thermo Fischer Scientific, Waltham, USA) was employed for the ionic content determination at the Hydrogeology Department of the University of Avignon, France. The analysis is considered valid for an ionic balance deviation of less than 5 %. Samples for $\delta^{18}\text{O}$ and $\delta^2\text{H}$ analysis were collected in 20 mL amber glass bottles avoiding any head-space. The measurements were performed with a liquid-water stable isotope analyzer DLT-100 (Los Gatos Research, San Jose, USA) according to the analytical scheme recommended by the International Atomic Energy Agency (Penna et al., 2010) at the Hydrogeology Department of the University of Corsica, France. The isotopic analysis is considered as valid for a standard deviation condition about 0.1 ‰ for $\delta^2\text{H}$ and 0.01 ‰ for $\delta^{18}\text{O}$. Samples for ^3H were collected in

0.5 L polyethylene and analyzed by electrolytic enrichment and liquid scintillation counting method according to Thatcher et al. (1977) at the Hydrogeology Department of the University of Avignon, France. Sampling for $^{14}\text{C}_{\text{DIC}}$ was performed on-site by precipitating water sample carbonates using barium chloride. The ^{14}C activity of the solid inorganic carbon obtained was determined by the liquid scintillation counting method after benzene synthesis according to Clark and Fritz (1997) at the Hydrogeology Department of the University of Avignon, France. Analysis for $^{87}\text{Sr}/^{86}\text{Sr}$ ratio was performed using a thermal ionization mass spectrometer (Finnigan MAT 262, Thermo Fischer Scientific, Waltham, USA) fitted with a multi-collector array consisting of five faraday cups. Corrections for mass fractionation were performed normalizing the $^{87}\text{Sr}/^{86}\text{Sr}$ ratio to the NBS 987 standard which value is 0.710250. These analyses were performed in the Department of Geological Sciences, at the University of Cape Town, South Africa.

4. Results and discussion

4.1. Recharge components identification

The river flow and the alluvial aquifer water level are strongly correlated with the monthly rainfall amount (Figure 2-A). Three peaks corresponding to high river water level events are observable in the alluvial aquifer during Nov-2018, Feb-2019, and Jun-19. The water level in the peatland appears quite stable but two peaks were recorded and correlate with the two high river water level events of Nov-2018 and Feb-2019. There is no time-lag between these events and the water level varies in the alluvial aquifer and the peatland on a monthly timescale. Except during summer, the EC in the peatland is generally lower than in the alluvial aquifer most likely due to a greater rainfall contribution. The high river water level events are always associated

201 with a decrease in the EC in the alluvial aquifer with values tending towards those
 202 observed in the peatland. This information coupled with the observation of the water
 203 level map (Figure 1) highlighting a clear continuity over the alluvial plain and the
 204 peatland area argue in favour of a strong groundwater-dependence of this peatland.
 205 Furthermore, the water level in the alluvial aquifer is generally higher than in the
 206 peatland, except during Aug-18 and Sept-18 (Figure 2-B). This highlights the
 207 contribution of other water bodies to recharge to the peatland and the possibility for
 208 the alluvial aquifer to be fed by the peatland.

209 Most of the samples from Aug-2018 and Dec-2018 plot along the Western
 210 Mediterranean Meteoric Water Line (WMMWL) of Celle-Jeanton et al. (2001)
 211 whereas those of May-2018, Feb-2019 and June-2019 plot closer to the Moltifau
 212 meteoric water line defined as $\delta^2\text{H} = 7.30 (\pm 0.49) \times \delta^{18}\text{O} + 7.37$ (OLSR approach; n
 213 $= 12$; $r^2 = 0.96$; Figure 3). No significant $\delta^{18}\text{O}$ enrichment is observed, indicating that
 214 evaporation processes are negligible despite the usual severe low precipitation
 215 period during the Mediterranean summer (Jasechko, 2019). Usually, water in
 216 peatland appears depleted in ^{18}O and ^2H during the high flow period and turns more
 217 enriched in $\delta^{18}\text{O}$ and $\delta^2\text{H}$ during the low flow period, typically due to the increase in
 218 atmospheric temperature and associated evaporation processes (Sprenger et al.,
 219 2017). However, in the setting of the present study the reverse is observed: the most
 220 enriched peatland water samples are found during Dec-2018 ($\delta^2\text{H}_{\text{mean}} = -50.5 \text{ ‰}$;
 221 $\delta^{18}\text{O}_{\text{mean}} = -8.11 \text{ ‰}$) and Feb-2019 ($\delta^2\text{H}_{\text{mean}} = -52.47 \text{ ‰}$; $\delta^{18}\text{O}_{\text{mean}} = -8.11 \text{ ‰}$), whereas
 222 the most depleted ones are found during May-2018 ($\delta^2\text{H}_{\text{mean}} = -63.7 \text{ ‰}$; $\delta^{18}\text{O}_{\text{mean}} = -$
 223 9.82 ‰), Jun-2019 ($\delta^2\text{H}_{\text{mean}} = -58.7 \text{ ‰}$; $\delta^{18}\text{O}_{\text{mean}} = -8.93 \text{ ‰}$), and Aug-2018 ($\delta^2\text{H}_{\text{mean}} =$
 224 -56.9 ‰ ; $\delta^{18}\text{O}_{\text{mean}} = -8.93 \text{ ‰}$). The most depleted peatland signatures are rather
 225 related to the colluvium, the granite, and the river samples than to the local rainfall

signature. Such depleted signatures may be explained by the influence of snowpack melting supplying the upstream river as previously measured ($\delta^2\text{H} = -85.7 \text{ ‰}$, $\delta^{18}\text{O} = -12.77 \text{ ‰}$) by van Geldern et al. (2014). Since the snowfall is significantly depleted in heavier isotopes compared to the summer rainfall, the average isotopic composition of snowpack remaining is also generally depleted despite the enrichment effect of sublimation and snowmelt (Beria et al., 2018). The snowpack melting, normally occurring in the watershed head during the spring and the beginning of the summer season, generates very depleted signatures into the river compared to the local rainfall that is then transferred into the peatland through the alluvial aquifer. To summarise, the $\delta^{18}\text{O}$ local framework revealed several potential contributors to recharge for the peatland: by the rain, a river, shallow groundwater from the colluvium, and by deep groundwater from the fractured granite.

4.2. Recharge component renewal dynamics

The amplitude of variation of the isotopic signature of the different recharge components highlights their renewal dynamics (Table 1). The local rainwater samples have elevated values about 10.12 ‰ for $\delta^{18}\text{O}$, and 8.5 TU for ^3H . The river has lower values about 1.90 ‰ for $\delta^{18}\text{O}$, and 2.4 TU for ^3H that are similar to the colluvium springs values of around 2.05 ‰ for $\delta^{18}\text{O}$, and 0.9 TU for ^3H . These values indicate homogenization of the local rainfall input within the colluvium reservoir. Nevertheless, to the extent that these sources dry up in summer, it can be concluded that the renewal of the colluvium reservoir is seasonal to annual. Lastly, the granite groundwater is the recharge component displaying longer renewal dynamics: ^3H values are always less than 0.5 TU and with a $^{14}\text{C}_{\text{DIC}}$ activity about 4.5 pMC, the groundwater residence time can be estimated to be around 25,500 years. Since no major $^{14}\text{C}_{\text{DIC}}$ source/sink within the granites may be expected, the groundwater age

estimation does not require correction and can be based solely on the radioactive decay of $^{14}\text{C}_{\text{DIC}}$ assuming piston flow from the recharge area to the sampling point F6. This estimate can be further validated against the stable isotope signature shift of about $\approx -2 \text{ ‰}$ for $\delta^{18}\text{O}$ and about $\approx -15 \text{ ‰}$ for $\delta^2\text{H}$ between the locally weighted mean isotope signature in rainfall and the granite groundwater revealing a clear paleo-climatic effect on a 25 K year scale. This shift is in the same order of magnitude as that observed in many aquifers hosting paleo-groundwater near the study site (Jiráková et al., 2011). Hence, the potential recharge contributions display a wide range of renewal dynamics: very fast for the local rainwater and the river, seasonal to annual for the colluvium springs, and up to millennial for the granite groundwater. During a full hydrological cycle, the $\delta^{18}\text{O}$ signatures of alluvial aquifer, peatland, and its outlets do not match with only one end-member (the local rainwater, the river, the granite groundwater, or the colluvium springs). They are usually between the river or the granite groundwater and the colluvium springs signatures, except during the summer when they are closer to the colluvium springs and the granite groundwater (Figure 4). These observations highlight complex mixing processes within the alluvial aquifer and the peatland. Furthermore, the isotopic signal within the alluvial aquifer, the peatland, and its outlets displays the same evolution pattern with comparable order of magnitude (Figure 4), implying a rapid water turnover within the peatland. Therefore, hydro-climatic conditions can potentially influence the seasonal recharge mechanisms (Figure 2), i.e. the mixing rates between the local rainfall, the river, the colluvium springs, and the granite groundwater over the seasons.

4.3. Quantification of the contribution of recharge components

4.3.1. Tracer choice

276 Peatlands hydrochemistry is usually complex and major ions can be expected to be
277 non-conservative especially due to redox conditions leading to processes such as
278 denitrification, or sulphate reduction (Bertrand et al., 2012). For the present study, it
279 is hypothesized that Na^+ , abundant and primarily granite-sourced (up to 116 mg/L in
280 F6), is one of the most conservative major ions and can be considered for mixing
281 proportions calculation. In contrast, fewer geochemical processes usually affect the
282 isotope tracers, making their interpretation less ambiguous than the simultaneous
283 changes in the geochemical content (Santoni et al., 2016). Given the location of the
284 study site within a strong altitudinal gradient watershed, it is possible to take
285 advantage of the resulting $\delta^{18}\text{O}$ signatures contrasts to discriminate the rainwater, the
286 river, the colluvium springs and the granite groundwater coming from varying
287 altitudes. Nevertheless, the $\delta^{18}\text{O}$ signatures may be ambiguous from a water body to
288 another one due to temporal variations, as this is the case for the river and the
289 granite groundwater or between the local rainwater and the colluvium springs (Figure
290 4).

291 To better discriminating these water bodies, the ^3H content can also be considered.
292 Over the past decades, natural ^3H variations in meteoric waters were masked by the
293 input of high levels of ^3H derived from atmospheric testing of thermonuclear
294 weapons. This anthropogenic ^3H has now largely decayed away leaving a natural
295 baseline level in precipitation. Excluding any source from nuclear energy power
296 plants, this natural baseline level in precipitation is principally controlled by
297 stratospheric production and fall-out rates, dilution from evaporation of oceanic water
298 and continental moisture recycling (Tadros et al., 2014; Juhlke et al., 2020). Like
299 stable isotopes of the water molecule, many so-called 'effects' may affect the
300 distribution of monthly integrated ^3H samples of precipitation. The seasonal effect is

likely to be the most pronounced in the present study and is characterised by increased ^3H contents during spring and early summer (Juhlke et al., 2020). As a consequence, and considering a half-life of 12.32 (± 0.02) years, the ^3H contents may be considered as a hydrological tracer of water origins at the sampling time step (month) of this study.

Coupled with $\delta^{18}\text{O}$, $^{87}\text{Sr}/^{86}\text{Sr}$ ratio is a very efficient tool to differentiate recharge components and calculate mixing proportions by avoiding inaccuracies due to hydrochemical processes (Santoni et al., 2016). In the present study, the $^{87}\text{Sr}/^{86}\text{Sr}$ analysis was conducted during a spring survey (June 2019) because the maximal dilution of the hydrosystem at this moment may result in a loss of hydrochemical signal for other tracers and thus potentially a source of mixing proportion calculation problems. The $^{87}\text{Sr}/^{86}\text{Sr}$ ratio is then expected to validate the mixing proportions calculated from using the Na^+ , $\delta^{18}\text{O}$, and ^3H tracers, which are easier tracers to implement but having specific limitations as explained earlier.

4.3.2. End-member mixing analysis settings

A end-member mixing analysis can be developed to explain the isotopic ($\delta^{18}\text{O}$, ^3H) and hydrochemical (Na^+) compositions of the alluvial aquifer and peatland water samples in terms of local rainwater, colluvium springs, granite groundwater and river water contribution for each season. According to Carrera et al. (2004), a four-member mixing model can be expressed by end-members as follows:

$$1 = f_a + f_b + f_c + f_d \quad (1)$$

$$[\text{X}]_{\text{sample}} = f_a \times [\text{X}]_{\text{rainwater}} + f_b \times [\text{X}]_{\text{colluvium}} + f_c \times [\text{X}]_{\text{granite}} + f_d \times [\text{X}]_{\text{river}} \quad (2)$$

where f refers to the relative fraction, subscripts a, b, c, and d refers to the selected end-members among the rainwater, the colluvium, the granite, and the river, and the $[\text{X}]$ can be either the Na^+ , $\delta^{18}\text{O}$, ^3H , or $^{87}\text{Sr}/^{86}\text{Sr}$ content. The end-members can be

characterized as follows (Table A1): (1) the rainwater as the quarterly weighted means of $\delta^{18}\text{O}$ at Moltifau. For the Na^+ , ^3H , and $^{87}\text{Sr}/^{86}\text{Sr}$ contents, data are respectively harvested from the Bonifacio, Corte, and Nîmes rain gauge stations close to the study site (Khaska et al., 2013; Santoni et al., 2016; Juhlke et al., 2020); (2) the sampling points R10 and R11 are considered as representative of the colluvium springs. During the Aug-2018 campaign, R10 and R11 springs were dry, the nearest sampling point R12 was then selected; (3) the sampling point F6 is considered as representative of the granite groundwater; (4) the upstream sampling point R18 is selected as representative of the river water. During the summer season, the sampling point distribution on the Na^+ , and ^3H vs $\delta^{18}\text{O}$ graphs (Figure 5) suggest the contribution of another recharge component within the peatland. According to Siegel et al. (1995), pore fluids may be flushed from peat during low water levels due to the decrease in the rainfall amount occurring in summer. In the present study, a 'peat' end-member needs then to be considered for the Aug-2018 campaign. Since pore fluids were not sampled, the Na^+ , $\delta^{18}\text{O}$, and ^3H values for the peat end-member are graphically determined also by an iterative process according to Hooper et al. (1990) to be 7.1 mg/L, -9.56 ‰, and 6.76, respectively (Table A1).

4.4. Mediterranean peatland recharge mechanisms

The results and interpretation of the EMMA are here presented for both the alluvial aquifer supplying the peatland and the peatland itself.

4.4.1. Spatial trends

In the alluvial aquifer, the proportion of local rainwater is maximal near the surface (75-88% at F8) and decreases with depth and distance to the riverbed. The proportion of river water is maximal close to the riverbed (58-92% at F1 and F3) and

decreases toward the Ciufellu granite massif. This is well supported by the piezometric map in Figure 1 and also in agreement with Genevier et al. (2014). The proportions of local rainwater and river decrease is compensated by an increase in the proportion of colluvium water in the vicinity of the Ciufellu granite massif (0-76% at F4) as well as by an increase in the proportion of granite groundwater with depth (20-62% at F7). The same trends are observed for the peatland water samples. T1 and T2 are more influenced by the river (36-82%), T4, and T6 by the colluvium springs (16-48%) and to a lesser extent by the granite groundwater (0-17%). All these mixing proportion calculations based on the Na^+ vs $\delta^{18}\text{O}$ vs ^3H approach is in very good agreement with those obtained with the $^{87}\text{Sr}/^{86}\text{Sr}$ vs $\delta^{18}\text{O}$ vs ^3H approach (Table A2). This can be explained by a strong altitude gradient and hydroclimatic seasonality influencing $\delta^{18}\text{O}$, and ^3H and by the lithology contrasts within the watershed influencing Na^+ and $^{87}\text{Sr}/^{86}\text{Sr}$ (Santoni et al., 2016). The only noticeable difference is that using the $^{87}\text{Sr}/^{86}\text{Sr}$ ratio allows a better detection and quantification of a low granite groundwater contribution to the peatland recharge. As an example, this contribution reaches 9 % at the T2 sampling point against 0 % using the Na content. As a consequence, even if the peatland is little extended, it appears as dependent on varied ground and surface water bodies. Nevertheless, since supplied by the alluvial aquifer and developing at the same water level, the peatland appears more influenced by the shallowest alluvial groundwater flow lines and by surface water bodies than by the deep granite groundwater flow lines.

4.4.2. Seasonal trends

A conceptual model of the recharge mechanisms in the peatland and the alluvial aquifer may be proposed for each season (Figure 6). In both the alluvial aquifer and

the peatland, the local rainwater and colluvium proportions are directly related to the rainfall scheme: the higher the rainfall amount is, the higher the proportions are. These proportions are maximal during fall (27% and 24%) and winter (32% and 28%), and minimal during spring (9% and 10%) and summer (4% and 12%). These results point out the peatland's dependence to water bodies different from the local rainfall. Furthermore, in both the alluvial aquifer and the peatland, proportions are related to the river flow: the higher the flow is, the higher the proportions is. These proportions are then maximal during fall (49%), winter (40%), and spring (81%). This means that the three main water level peaks observed in the alluvial aquifer after the fall and winter floods as well as after the snowpack melting in the high watershed part during spring contribute mainly to the recharge. Moreover, as explained in the spatial trends section, the granite groundwater proportion varies in space but appears season-dependent. Within the alluvial aquifer, the proportion is maximal during summer, decreases in fall, and is minimal in winter and spring. This means that the higher the local rainwater, the colluvium springs, and the river contributions are, the higher the dilution of the granite groundwater recharge component is. Within the peatland, the granite groundwater recharge component is noticeable only during summer (up to 16%, with a mean about 4 %), the peat pore water being the most representative component due to the water reservoir function of the peatland. Based on these observations, it is possible to establish a recharge component succession from one season to another. The high watershed river is the first recharge component involved. The rain and the shallow flow through the mountainside colluvium constitute subsequently the second recharge component providing support during drier periods. The granite groundwater constitutes the fourth and last recharge component able to supply the peatland during summer throughout the alluvial aquifer. During summer,

the peatland continues to be fed by the alluvial aquifer (Figure 2). However, during the summer low precipitation period, the peatland seems to support the flow of the alluvial aquifer downstream, as shown by the chemistry of alluvial groundwater (Figure 5) and the inversion of water tables (Figure 2B).

4.5. From hydrogeological resilience to the vulnerability of Mediterranean peatlands

At first glance, the peatland's hydrogeological resilience to climate change appears limited because the river-alluvial aquifer system on which the peatland depends is highly responsive to the seasonality of hydroclimatic conditions. In particular, there is no significant time lag between the rain events and the alluvial aquifer water level response supplying the peatland. This finding testifies to the high reversibility of the peatland hydrological status and vulnerability to low precipitation period during the Mediterranean summer. However, the peatland has proven to be resilient during the low precipitation period, as shown by the water level monitoring (Figure 2). This can be explained by the reservoir function of the peat (pore water) and by the multiple groundwater sources supplying the peatland, making it not solely dependent on precipitation feeding into the alluvial aquifer and the river. The peatland benefits from low but perennial inflows from reservoirs with longer renewal dynamics (colluvium and granite groundwater) as well as from the more important but very short time inflows from summer storms governing the river flow.

The hydrogeological functioning of Mediterranean peatlands is an intrinsic asset making them well adapted to the Mediterranean climate. From a qualitative point of view, groundwater bodies with long renewal dynamics constitute perennial and presumed good quality recharge components. However, their connection with surface

water bodies makes them vulnerable to any land-use changes likely to affect water quality and quantity within the watershed: population and urban growth (drinking water supply, sanitation), agricultural practices (irrigation, fertilizers, phytosanitary products) as this is more widely the case in the Mediterranean. During the summer low precipitation period, the river, the colluvium, and the granite groundwater may be insufficient to maintain a sufficient water level in the alluvial aquifer to support peatland hydrological functioning, leading to a water table inversion (Figure 2B). During such unfavourable hydrological conditions, the peatland survival relies on the peat reservoir function. This demonstrates the precarious hydrogeological equilibrium within the peatland. Any increase in the water table inversion duration can then lead to the peatland drying up. Critically, the drying up of peatland, even temporarily, is likely to permanently alter the plant and animal species it contains. As a consequence, any slight external pressure on the alluvial groundwater level from abstractions to support irrigation and drinking water supply, or through climate change (by increasing the temperature or the drought length, and decreasing or modifying the rainfall scheme) can result in the drying up, where the worst-case scenario is complete desiccation.

4.6. Implications on peatlands sustainable management strategies in the Mediterranean region

The Moltifau peatland can be considered a representative peatland from the western Mediterranean region at low altitude, where worsening vulnerability to drought conditions has been documented (Parish et al., 2008). As part of the territory of France, one of the Mediterranean rim countries offering the strictest legislative

450 framework in favour of wetlands preservation, the peatland provides an important
451 perspective on deficiencies in the legislation and management of such ecosystems.

452 At the peatland scale, management strategies are theoretically developed to
453 preserve its ecological value. Nevertheless, the lack of willingness, financial
454 resources as well as the involvement of several environmental institutions such as
455 the French national forestry board (ONF) and the Directorate of the Environment
456 (DREAL) make policies ineffective. Added to this are potential administrative
457 difficulties that might arise through the transfer of wetland management strategies to
458 the local authorities through the Regional Environmental Office (OEC). This situation
459 is due to the State decentralization which recognizes the Corsica administrative
460 Region as fully in charge of environmental management and conservation, blurring
461 the situation and making coordination even more complicated from the European to
462 the local level.. Furthermore, the preservation strategy presently developed only
463 deals with biodiversity aspects and is applied only within the strict area of the
464 peatland. None of the strategies takes into account the need to preserve the water
465 body it contains and those inter-connected to it in a wider context. Indeed, the
466 peatland water body does not appear in any management document for aquatic
467 environments related to the local transcription of the European Water Framework
468 Directive of 2000 (WFD, 2000/60/EC). The fate of the peatland is therefore in the
469 hands of the local authorities who are forced to reach compromises between the
470 peatland ecosystem services preservation, and the necessary socio-economic
471 development of the territory. Due to its small size and lack of visibility, both in the
472 landscape (no barriers, signage, or other physical materialization) and in the minds
473 (little communication and education about its ecological value), this peatland is
474 suffering from increasing human pressure.

475 The WFD is widely accepted as the most ambitious and substantial European
476 sustainable development legislation to date. By nature, the WFD aims at reaching
477 qualitative and quantitative “good status” for identified surface and groundwater
478 bodies supplying wetlands by the end of the second or third management cycles
479 extending during 2015-2012 and 2021 to 2027, respectively. Although this approach
480 attempts to address the most serious health-threatening impacts on the environment,
481 many wetlands of international importance remain outside the WFD. On the one
482 hand, as the number of water bodies is defined according to political criteria, most
483 often in the way to reduce costs (Moss, 2008), the managed groundwater body size
484 covers generally wide areas, unadapted for the preservation of small and scattered
485 Mediterranean peatlands. As an example, the Moltifau peatland represents less than
486 1/80,000 of the groundwater body's total size. On the other hand, pollution sources
487 being often multiple in nature and difficult to constrain due to the complexity of
488 human activities on the territory, basic measurements for water body quality
489 indicators as established in the WFD appear insufficient to assess pressure and
490 impact, leading to a misunderstanding of the water bodies status (Voulvoulis et al.,
491 2017).

492 As demonstrated in this study, Mediterranean peatlands are groundwater-dependent
493 (GDE) and well connected to the whole hydrographic network. In its present form, the
494 WFD requires the establishment of separate Programmes of Measures (PoMs) for
495 groundwater and surface water bodies without taking into account the complex
496 hydrological functioning of such transitional environments. Water flow connects the
497 different components of the peatland with the whole watershed area, making them
498 particularly vulnerable to a wide range of human-induced impacts. This specificity
499 requires planning of PoMs, not at a water body scale, but at the hydrosystem scale

500 by understanding the relationship between land and water under different socio-
501 economic drivers (Varela-Ortega et al., 2011; Vlachopoulou et al., 2014). Such an
502 integrated and coordinated approach should be implemented in the WFD by the
503 establishment of appropriate policy for inland GDE such as Mediterranean peatlands.
504 This implies a knowledge gain to define around the hydrosystem an area called
505 "optimal functioning conditions zone", identifying and coordinating the people acting
506 over the relevant territory, and finally identifying relevant indicators for evaluating the
507 status of the hydro-ecosystem (Carvalho et al., 2019). Encouraged by cooperation
508 projects, several UE and non-UE countries of the Mediterranean rim successfully
509 initiated the Integrated Water Resources Management, mainly focusing on highly
510 anthropized and regional river basins (Tavakoly et al., 2019). On a smaller scale, as
511 is the case for the Moltifau peatland, it is difficult to implement this approach because
512 of the lack of willingness and coordination between all environmental institutions and
513 land users. A solution would be to propose the concept of scientifically-piloted PoMs
514 at the hydro-ecosystem level for the third WFD cycle (2021-2027). Based on the
515 present study, its delimitation would be based on the peatland's "optimal functioning
516 conditions zone" including both surface and groundwater. Quality indicators would
517 facilitate assessment of the whole ecosystem status, including new groundwater
518 degradation trends and impacts on GDEs by the implementation of relevant research
519 tools such as the monitoring of water levels, physico-chemical parameters,
520 hydrochemistry, and isotopes (Erostate et al., 2020). The advantage of this proposal
521 is also the consideration of heterogeneities in hydroclimatic conditions and
522 groundwater contribution at seasonal and inter-annual timescales in the context of
523 increasing human and climate pressures threatening more and more the peatlands,
524 one of the main biodiversity hotspots within the Mediterranean.

525

526 **5. Conclusion**

527 This study represents one of the first comprehensive analyses of the seasonal
528 recharge mechanisms of a representative Mediterranean peatland, integrating a
529 range of geochemical and isotope hydrology tools (Na^+ , $\delta^{18}\text{O}$, ^3H , $^{87}\text{Sr}/^{86}\text{Sr}$). Such an
530 approach is relevant to identify and quantify complex water flows supplying
531 Mediterranean peatlands and could be adopted in other peatlands worldwide
532 potentially connected to multiple surface and groundwater bodies. This study
533 confirmed the groundwater-dependent status of Mediterranean peatlands,
534 emphasizing the strong seasonal heterogeneity of the recharge component
535 contributions despite a very stable water level throughout the year. Peatlands are
536 dependent on surface and shallow flows during fall, winter, and spring, and are highly
537 dependent on shallow and deep groundwater during summer. This important finding
538 suggests, on the one hand, an intrinsic resilience to low precipitation period during
539 the Mediterranean summer and on the other hand, the connectivity between all
540 surface and groundwater bodies of the watershed. This important hydrological
541 functioning makes the peatlands vulnerable to any change in land use within the
542 watershed or in hydroclimatic conditions as expected in the context of global change.
543 The peatland vulnerability is also increased by poor consideration of their specific
544 functioning into water and aquatic environment management policies such as the
545 European WFD. A paradigm-shift with management based on the hydrosystem
546 concept is necessary and implies a downscaling adapted to Mediterranean peatlands
547 size and their transitional situation connecting surface and groundwater. Aquatic
548 environments, surface, and groundwater bodies currently being managed
549 independently, need to be coordinated and efforts between environmental institutions

and land users need to be improved to define "optimal functioning conditions" based on new quality indicators to enhance and maintain Mediterranean peatlands ecosystem services.

References

- Beria, H., Larsen, J.R., Ceperley, N.C., Michelon, A., Vennemann, T. and Schaepli, B. 2018. Understanding snow hydrological processes through the lens of stable water isotopes. Wiley Interdisciplinary Reviews: Water 5(6), e1311. <https://doi.org/10.1002/wat2.1311>
- Bertrand, G., Goldscheider, N., Gobat, J.-M. and Hunkeler, D. 2012. From multi-scale conceptualization to a classification system for inland groundwater-dependent ecosystems. Hydrogeology Journal 20(1), 5-25. <https://doi.org/10.1007/s10040-011-0791-5>
- Burguet-Moretti, A., Petrera, C. and Culioli, J. 2011. Fiche descriptive sur les zones humides Ramsar (FDR), tourbière de Moltifao, Corse, France. RAMSAR 2009-2012 version. <https://rsis.ramsar.org/ris/1994>
- Carrera, J., Vázquez-Suñé, E., Castillo, O. and Sánchez-Vila, X. 2004. A methodology to compute mixing ratios with uncertain end-members. Water resources research 40(12). <https://doi.org/10.1029/2003WR002263>
- Carvalho, L., Mackay, E.B., Cardoso, A.C., Baattrup-Pedersen, A., Birk, S., Blackstock, K.L., Borics, G., Borja, A., Feld, C.K. and Ferreira, M.T. 2019. Protecting and restoring Europe's waters: An analysis of the future development needs of the Water Framework Directive. Science of the Total Environment 658, 1228-1238. <https://doi.org/10.1016/j.scitotenv.2018.12.255>
- Celle-jeanton, H., Travi, Y. and Blavoux, B. 2001. Isotopic typology of the precipitation in the Western Mediterranean region at three different time scales. Geophysical Research Letters 28(7), 1215-1218. <https://doi.org/10.1029/2000GL012407>
- Clark, I.D. and Fritz, P. (1997) Environmental Isotopes in Hydrogeology, CRC Press/Lewis Publishers, Boca Raton, FL.
- Craig, H. 1961. Isotopic variations in meteoric waters. Science 133(3465), 1702-1703. <https://doi.org/10.1126/science.133.3467.1833>
- Erostate, M., Huneau, F., Garel, E., Ghiotti, S., Vystavna, Y., Garrido, M. and Pasqualini, V. 2020. Groundwater dependent ecosystems in coastal Mediterranean regions: Characterization, challenges and management for their protection. Water Research 172, 115461. <https://doi.org/10.1016/j.watres.2019.115461>
- Finlayson, C.M., Milton, G.R., Prentice, R.C. and Davidson, N.C. (2018) The Wetland Book: II: Distribution, Description, and Conservation, Springer.
- Gardner, R.C., Finlayson, C.M. and *al.*, e. 2018. Perspectives mondiales des zones humides : état des zones humides à l'échelle mondiale et des services qu'elles fournissent à l'humanité. Secrétariat de la Convention de Ramsar, Gland, Suisse.
- Genevier, M., Frissant, N., Tirmont, M., Auterives, C., Tissoux, H. and Bodéré, G. 2014. Tourbière de Valdu, Moltifao (2B) : structure, fonctionnement et sensibilité à l'érosion des berges de l'Asco. BRGM Rapport final BRGM/RP-63922-FR 1, 132(1), 132. <http://infoterre.brgm.fr/rapports/RP-63922-FR.pdf>
- Hettiarachchi, M., Morrison, T.H. and McAlpine, C. 2015. Forty-three years of Ramsar and urban wetlands. Glob. Environ. Change-Human Policy Dimens. 32, 57-66. <https://doi.org/10.1016/j.gloenvcha.2015.02.009>
- Hooper, R.P., Christophersen, N. and Peters, N.E. 1990. Modelling streamwater chemistry as a mixture of soilwater end-members—An application to the Panola Mountain catchment,

- Georgia, USA. *Journal of Hydrology* 116(1-4), 321-343. [https://doi.org/10.1016/0022-1694\(90\)90131-G](https://doi.org/10.1016/0022-1694(90)90131-G)
- Howie, S.A. and Van Meerveld, H. 2013. Regional and local patterns in depth to water table, hydrochemistry and peat properties of bogs and their laggs in coastal British Columbia. *Hydrology and Earth System Sciences* 17(9), 3421-3435. <https://doi.org/10.5194/hess-17-3421-2013>
- Huang, X., Pancost, R.D., Xue, J., Gu, Y., Evershed, R.P. and Xie, S. 2018. Response of carbon cycle to drier conditions in the mid-Holocene in central China. *Nature communications* 9(1), 1-9. <https://doi.org/10.1038/s41467-018-03804-w>
- Isokangas, E., Rossi, P.M., Ronkanen, A.K., Marttila, H., Rozanski, K. and Kløve, B. 2017. Quantifying spatial groundwater dependence in peatlands through a distributed isotope mass balance approach. *Water Resources Research* 53(3), 2524-2541. <https://doi.org/10.1002/2016WR019661>
- Jasechko, S. 2019. Global isotope hydrogeology—Review. *Reviews of Geophysics* 57(3), 835-965. <https://doi.org/10.1029/2018RG000627>
- Jiráková, H., Huneau, F., Celle-Jeanton, H., Hrkál, Z. and Le Coustumer, P. 2011. Insights into palaeorecharge conditions for European deep aquifers. *Hydrogeology Journal* 19(8), 1545-1562. <https://doi.org/10.1007/s10040-011-0765-7>
- Juhlke, T.R., Sültenfuß, J., Trachte, K., Huneau, F., Garel, E., Santoni, S., Barth, J.A. and van Geldern, R. 2020. Tritium as a hydrological tracer in Mediterranean precipitation events. *Atmospheric Chemistry & Physics* 20(6). <https://doi.org/10.5194/acp-20-3555-2020>
- Khaska, M., La Salle, C.L.G., Lancelot, J., Mohamad, A., Verdoux, P., Noret, A. and Simler, R. 2013. Origin of groundwater salinity (current seawater vs. saline deep water) in a coastal karst aquifer based on Sr and Cl isotopes. Case study of the La Clape massif (southern France). *Applied geochemistry* 37, 212-227. <https://doi.org/10.1016/j.apgeochem.2013.07.006>
- Kløve, B., Ala-Aho, P., Bertrand, G., Boukalova, Z., Ertürk, A., Goldscheider, N., Ilmonen, J., Karakaya, N., Kupfersberger, H. and Kværner, J. 2011. Groundwater dependent ecosystems. Part I: Hydroecological status and trends. *Environmental Science & Policy* 14(7), 770-781. <https://doi.org/10.1016/j.envsci.2011.04.002>
- Malek, Ž., Verburg, P.H., Geijzendorffer, I.R., Bondeau, A. and Cramer, W. 2018. Global change effects on land management in the Mediterranean region. *Global Environmental Change* 50, 238-254
- Moss, B. 2008. The Water Framework Directive: total environment or political compromise? *Science of the total environment* 400(1-3), 32-41. <https://doi.org/10.1016/j.scitotenv.2008.04.029>
- Parish, F., Sirin, A., Charman, D., Joosten, H., Minayeva, T., Silvius, M. and Stringer, L. 2008. Assessment on Peatlands, Biodiversity and Climate Change : Main Report. Global Environment Centre, Kuala Lumpur and Wetlands International, Wageningen
- Peel, M.C., Finlayson, B.L. and McMahon, T.A. 2007. Updated world map of the Köppen-Geiger climate classification. *Hydrol. Earth Syst. Sci.* 11(1633–1644). <https://doi.org/10.5194/hess-11-1633-2007>
- Penna, D., Stenni, B., Šanda, M., Wrede, S., Bogaard, T., Gobbi, A., Borga, M., Fischer, B., Bonazza, M. and Chárová, Z. 2010. On the reproducibility and repeatability of laser absorption spectroscopy measurements for $\delta^2\text{H}$ and $\delta^{18}\text{O}$ isotopic analysis. *Hydrology and Earth System Sciences* 14(8), 1551-1566. <https://doi.org/10.5194/hess-14-1551-2010>
- Poher, Y. 2017. Dynamique de la biodiversité et changements environnementaux en Corse depuis 7000 ans: éclairages paléontologiques et paléobotaniques. Thèse de Doctorat de l'Université d'Aix-Marseille. <http://www.theses.fr/2017AIXM0435>
- Reille, M. 1997. Analyse pollinique des tourbières de Valdo et Baghietto (commune de Moltifao, Haute-Corse). . Programme Life "conservation des habitats naturels et des espèces végétales d'intérêt communautaire prioritaire de la Corse" 1, 1-13. <https://doi.org/10.3406/quate.1988.1881>

- Rossi, P., Durand-Delga, M., Carnon, J.-M., Guieu, G., Conchon, O., Libourel, G., Loye-Pilot, M.-D., Ollé, J.-J., Pequignot, G., Potdevin, J.-L., Rieuf, M., Rodriguez, G., Sedan, O., Vellutini, P.-J. and Rouire, J. 1994. Carte géologique de la France (1/50000), Feuille de Corte (1110). Orléans : BRGM
- Santoni, S., Huneau, F., Garel, E., Aquilina, L., Vergnaud-Ayraud, V., Labasque, T. and Celle-Jeanton, H. 2016. Strontium isotopes as tracers of water-rocks interactions, mixing processes and residence time indicator of groundwater within the granite-carbonate coastal aquifer of Bonifacio (Corsica, France). *Science of the Total Environment* 573, 233-246. <https://doi.org/10.1016/j.scitotenv.2016.08.087>
- Santoni, S., Huneau, F., Garel, E. and Celle-Jeanton, H. 2018. Multiple recharge processes to heterogeneous Mediterranean coastal aquifers and implications on recharge rates evolution in time. *Journal of Hydrology* 559, 669-683. <https://doi.org/10.1016/j.jhydrol.2018.02.068>
- Siegel, D., Reeve, A., Glaser, P.H. and Romanowicz, E. 1995. Climate-driven flushing of pore water in peatlands. *Nature* 374(6522), 531-533. <https://doi.org/10.1038/374531a0>
- Sprenger, M., Tetzlaff, D., Tunaley, C., Dick, J. and Soulsby, C. 2017. Evaporation fractionation in a peatland drainage network affects stream water isotope composition. *Water Resources Research* 53(1), 851-866. <https://doi.org/10.1002/2016WR019258>
- Tadros, C.V., Hughes, C.E., Crawford, J., Hollins, S.E. and Chisari, R. 2014. Tritium in Australian precipitation: A 50 year record. *Journal of hydrology* 513, 262-273. <https://doi.org/10.1016/j.jhydrol.2014.03.031>
- Tavakoly, A.A., Habets, F., Saleh, F., Yang, Z.-L., Bourgeois, C. and Maidment, D.R. 2019. An integrated framework to model nitrate contaminants with interactions of agriculture, groundwater, and surface water at regional scales: The STICS–EauDyssée coupled models applied over the Seine River Basin. *Journal of Hydrology* 568, 943-958. <https://doi.org/10.1016/j.jhydrol.2018.11.061>
- Thatcher, L.L., Janzer, V.J. and Edwards, K.W. (1977) Methods for determination of radioactive substances in water and fluvial sediments, US Government Printing Office.
- Urák, I., Hartel, T., Gallé, R. and Balog, A. 2017. Worldwide peatland degradations and the related carbon dioxide emissions: the importance of policy regulations. *Environmental Science & Policy* 69, 57-64. <https://doi.org/10.1016/j.envsci.2016.12.012>
- van Geldern, R., Kuhlemann, J., Schiebel, R., Taubald, H. and Barth, J.A. 2014. Stable water isotope patterns in a climate change hotspot: the isotope hydrology framework of Corsica (western Mediterranean). *Isotopes in environmental and health studies* 50(2), 184-200. <https://doi.org/10.1080/10256016.2013.839559>
- Varela-Ortega, C., Blanco-Gutierrez, I., Swartz, C.H. and Downing, T.E. 2011. Balancing groundwater conservation and rural livelihoods under water and climate uncertainties: An integrated hydro-economic modeling framework. *Glob. Environ. Change-Human Policy Dimens.* 21(2), 604-619. <https://doi.org/10.1016/j.gloenvcha.2010.12.001>
- Vlachopoulou, M., Coughlin, D., Forrow, D., Kirk, S., Logan, P. and Voulvoulis, N. 2014. The potential of using the ecosystem approach in the implementation of the EU Water Framework Directive. *Science of the Total Environment* 470, 684-694. <https://doi.org/10.1016/j.scitotenv.2013.09.072>
- Voulvoulis, N., Arpon, K.D. and Giakoumis, T. 2017. The EU Water Framework Directive: From great expectations to problems with implementation. *Science of the Total Environment* 575, 358-366. <http://dx.doi.org/10.1016/j.scitotenv.2016.09.228>

List of Figures (color should not be used for any figures in print)

Figure 1: Map of the study site with the sampling point network, geology, and potentiometric levels.

Figure 2: Time series of water level and EC parameters within the peatland (T4) and the alluvial aquifer (F4) compared with the local monthly rainfall amount and with the monthly river flow from May-2018 to Jul-2019 (A) with a particular focus on water levels in the peatland and the alluvial aquifer during the summer (B).

Figure 3: $\delta^2\text{H}$ vs $\delta^{18}\text{O}$ plot of all water samples. The GMWL is the Global Meteoric Water Line after Craig (1961), the WMMWL is the Western Mediterranean Meteoric Water Line after Celle-Jeanton et al. (2001) and the LMWL is the Local Meteoric Water Line in Moltifau. The river water sample for the watershed head is given in van Geldern et al. (2014).

Figure 4: Seasonal evolution of $\delta^{18}\text{O}$ signatures within the alluvial aquifer, the peatland, and its outlets according to the monthly rainfall amount, the monthly river flow and the local isotopic framework (local rainwater, river, granite groundwater, and colluvium springs) during a full hydrological cycle.

Figure 5: Na^+ , ^3H , and $^{87}\text{Sr}/^{86}\text{Sr}$ vs d^{18}O plots of the alluvial aquifer and peatland samples for the fall, winter, spring, and summer campaigns according to the local rainwater, river, Colluvium springs and granite groundwater end-members.

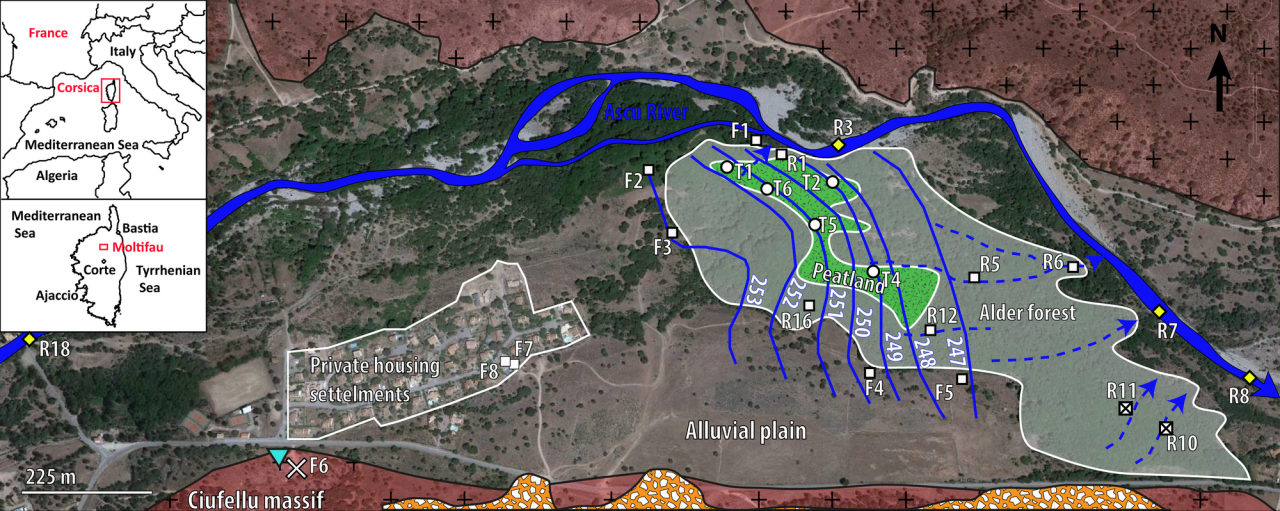
Figure 6: Conceptual model showing the quantification of seasonal variation of the contribution of water recharge components in the Mediterranean peatland. The pie chart indicates the quantification of seasonal variation of the contribution of water recharge components in the alluvial aquifer.

List of Tables

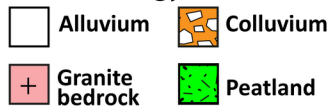
Table 1: Amplitude of variation of $\delta^{18}\text{O}$, and ^3H in the rainwater, the river, the colluvium springs and in the granite groundwater. The $^{14}\text{C}_{\text{DIC}}$ age is also given for the granite groundwater.

Table A1 (supplementary material): Na^+ , ^3H , $\delta^{18}\text{O}$, and $^{87}\text{Sr}/^{86}\text{Sr}$ values for each end-member (local rainwater, colluvium, granite, river, peat) and each season (May-18, Aug-18, Dec-18, Feb-19, and Jun-19). Rainwater Na^+ , ^3H , and $^{87}\text{Sr}/^{86}\text{Sr}$ contents are harvested from Santoni et al. (2018), Juhlke et al. (2020), and Khaska et al. (2013), respectively.

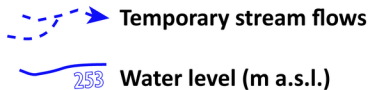
Table A2 (supplementary material): Peatland and alluvial aquifer mixing rates computed from Na^+ , $\delta^{18}\text{O}$, and ^3H data in terms of local rainwater, colluvium springs, granite groundwater, river, and peat contribution for the Aug-18, Dec-18, Feb-19, and Jun-19 campaigns. In parenthesis, mixing rates computed from $^{87}\text{Sr}/^{86}\text{Sr}$, $\delta^{18}\text{O}$, and ^3H data.



Lithology

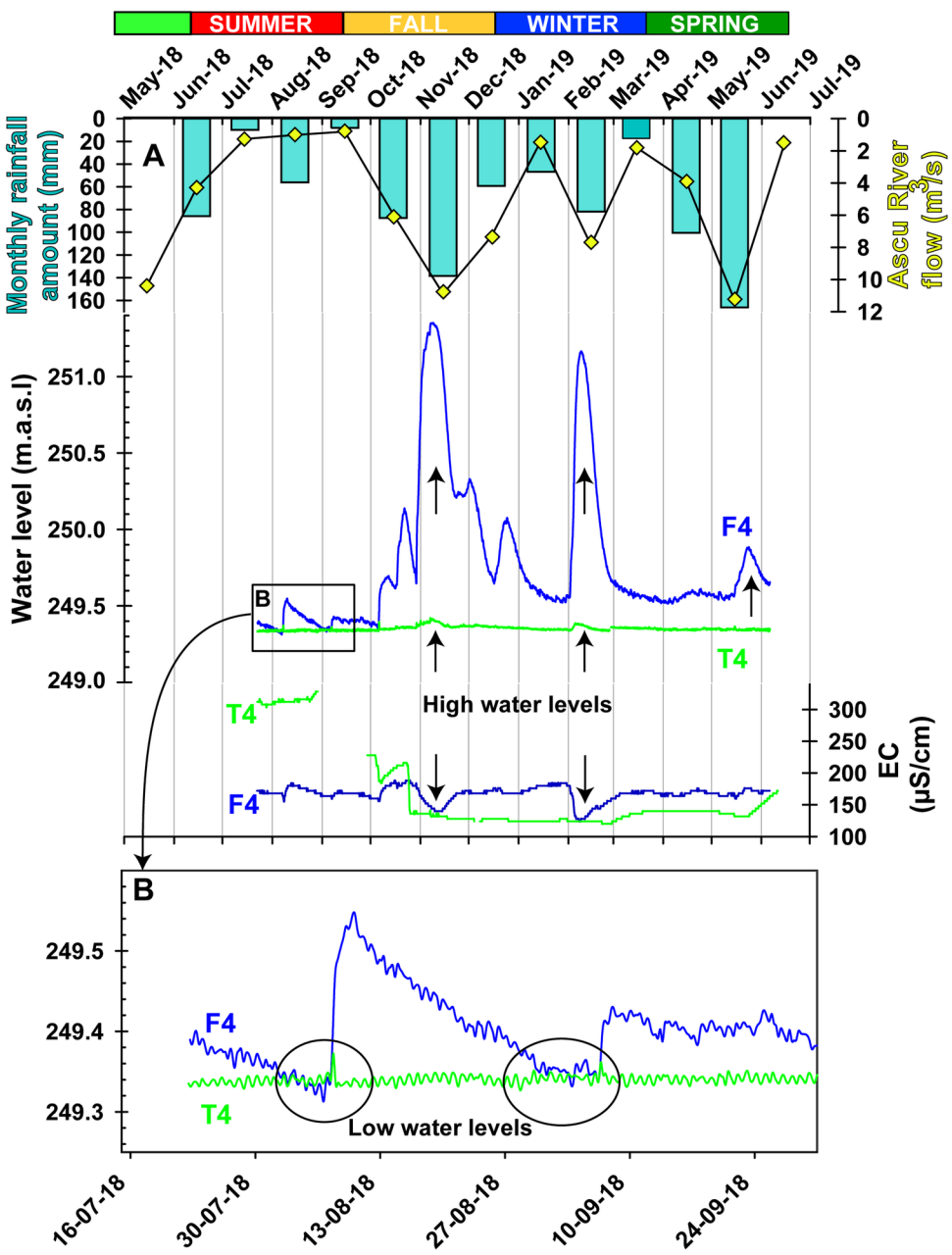


Hydrology and hydrogeology

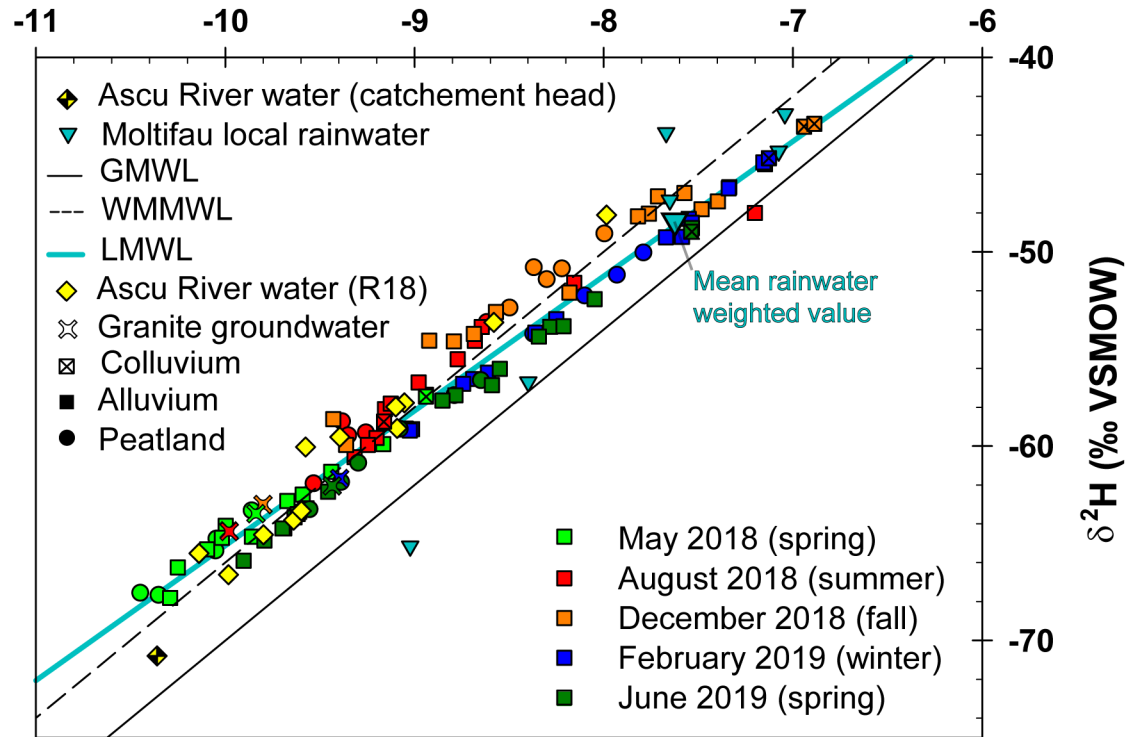


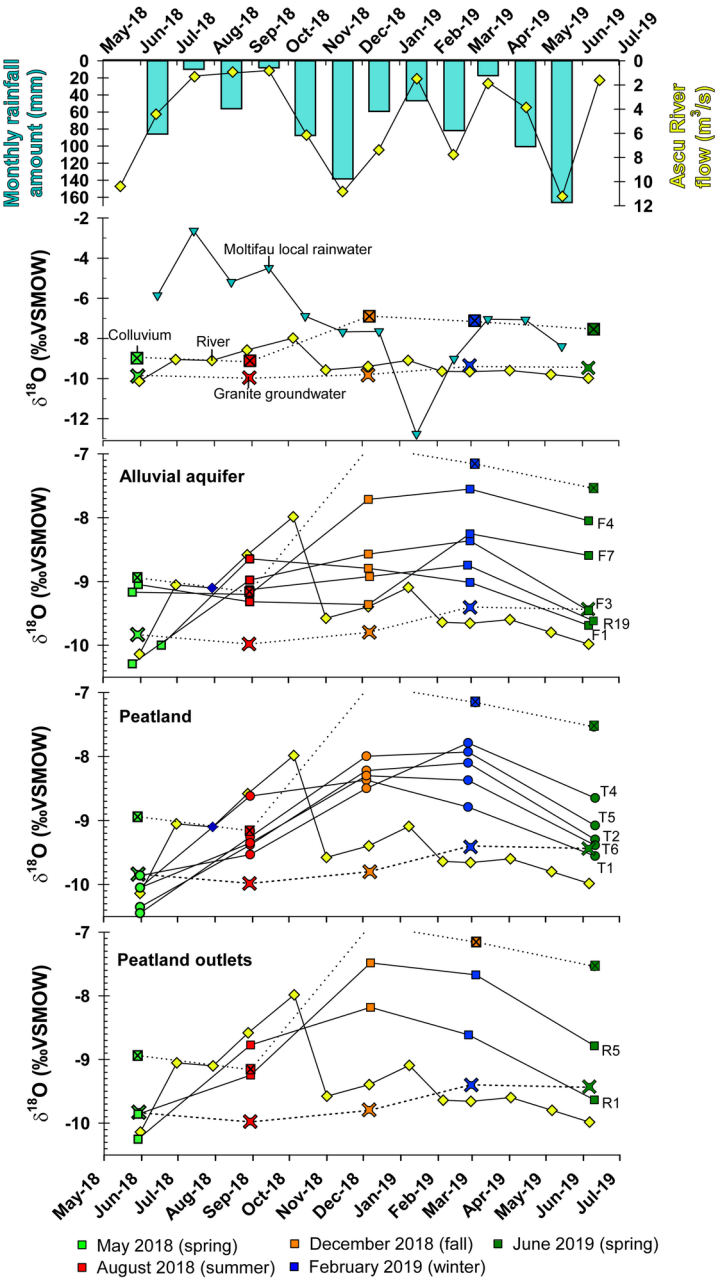
Sampling network

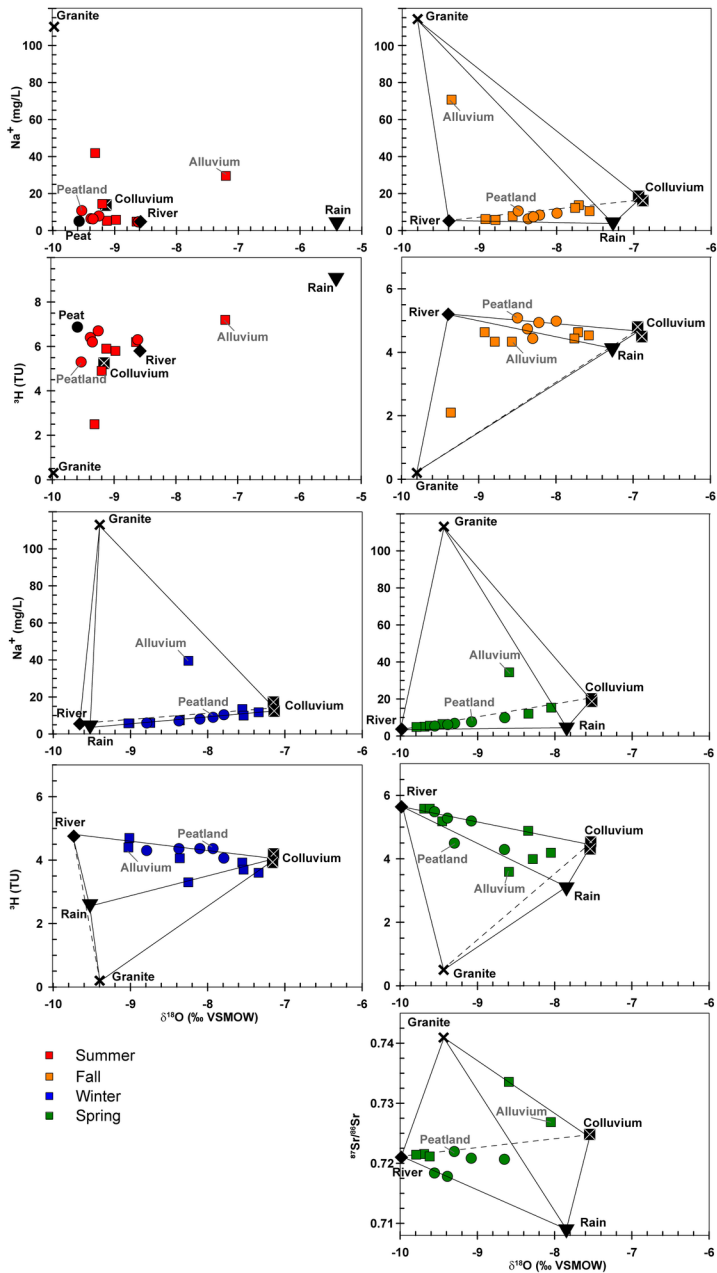




$\delta^{18}\text{O}$ (‰ VSMOW)







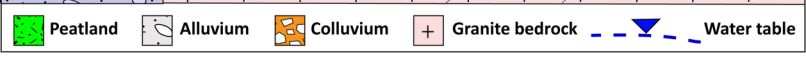
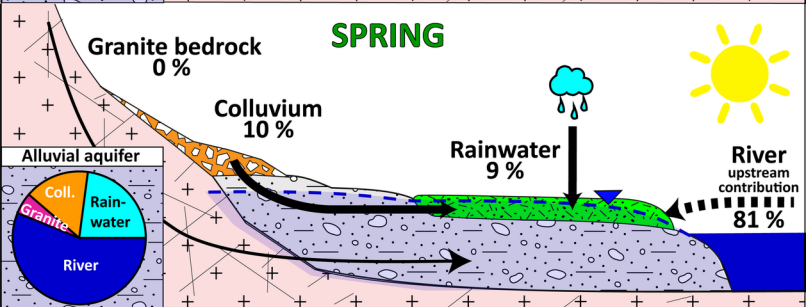
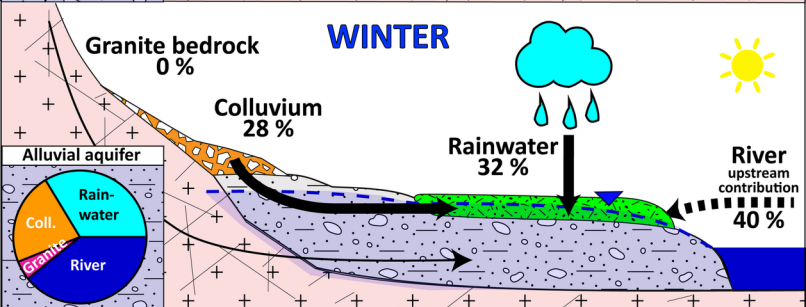
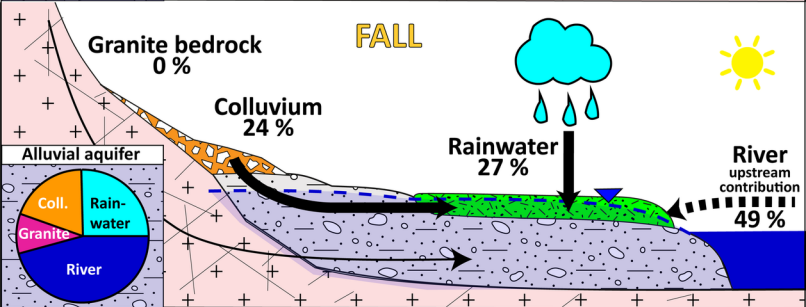
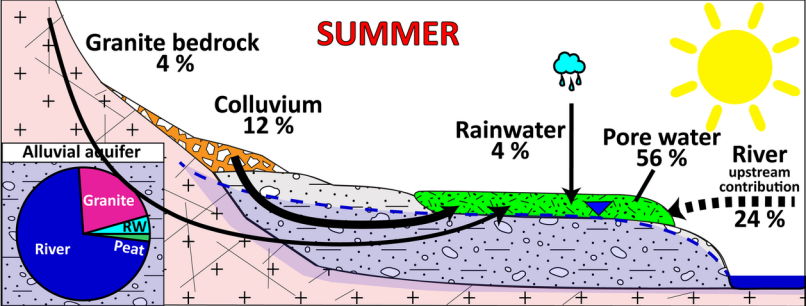


Table 1: Amplitude of variation of $\delta^{18}\text{O}$, and ^3H in the local rainwater, the Ascu River, the colluvium springs and in the granite groundwater. The $^{14}\text{C}_{\text{DIC}}$ age is also given for the granite groundwater.

		$\delta^{18}\text{O}$ (‰ VSMOW)	^3H (TU)	^{14}C age (years)
Local rainwater	min	-12.76	1.6	
	max	-2.64	10.1	
	max-min	10.12	8.5	
Ascu River	min	-10.25	4.0	
	max	-8.35	6.4	
	max-min	1.90	2.4	
Colluvium springs	min	-8.94	3.9	
	max	-6.89	4.8	
	max-min	2.05	0.9	
Granite groundwater	min	-9.98		
	max	-9.40	0.5	25,500
	max-min	0.58		

